Graphene-assisted quasi-van der Waals epitaxy of AlN film for ultraviolet light emitting diodes on nano-patterned sapphire substrate Ⓕ

Hongliang Chang ⓘD, Zhaolong Chen, Weijiang Li, Jianchang Yan, Rui Hou, Shenyuan Yang, Zhiqiang Liu ⓘD, Guodong Yuan ⓘD, Junxi Wang, Jinmin Li, Peng Gao, and Tongbo Wei ⓘD

COLLECTIONS

Ⓕ This paper was selected as Featured

View Online   Export Citation   CrossMark

Graphene-assisted quasi-van der Waals epitaxy of AlN film for ultraviolet light emitting diodes on nano-patterned sapphire substrate

Hongliang Chang,[1,2,a] Zhaolong Chen,[3,a] Weijiang Li,[1,2] Jianchang Yan,[1,2] Rui Hou,[2,4] Shenyuan Yang,[2,4,b] Zhiqiang Liu,[1,2] Guodong Yuan,[1,2] Junxi Wang,[1,2] Jinmin Li,[1,2] Peng Gao,[3,5,b] and Tongbo Wei[1,2,b]

AFFILIATIONS

[1]Research and Development Center for Semiconductor Lighting Technology, Institute of Semiconductors, Chinese Academy of Sciences, Beijing 100083, China
[2]Center of Materials Science and Optoelectronics Engineering, University of Chinese Academy of Sciences, Beijing 100049, China
[3]Center for Nanochemistry, Beijing Science and Engineering Center for Nanocarbons, College of Chemistry and Molecular Engineering, Peking University, Beijing 100871, China
[4]State Key Laboratory of Superlattices and Microstructures, Institute of Semiconductors, Chinese Academy of Sciences, Beijing 100083, China
[5]International Center for Quantum Materials, and Electron Microscopy Laboratory, School of Physics, Peking University, Beijing 100871, China

[a]Contributions: H. Chang and Z. Chen contributed equally to this work.
[b]Electronic addresses: tbwei@semi.ac.cn, p-gao@pku.edu.cn, and syyang@semi.ac.cn.

ABSTRACT

We report the growth of high-quality AlN films on nano-patterned sapphire substrates (NPSSs) by graphene-assisted quasi-van der Waals epitaxy, which enables rapid coalescence to shorten the growth time. Due to the presence of graphene (Gr), AlN tends to be two-dimensional laterally expanded on the NPSS, leading to the reduction of dislocation density and strain release in the AlN epitaxial layer. Using first-principles calculations, we confirm that Gr can reduce the surface migration barrier and promote the lateral migration of metal Al atoms. Furthermore, the electroluminescence results of deep ultraviolet light emitting diodes (DUV-LEDs) have exhibited greatly enhanced emission located at 280 nm by inserting the Gr interlayer. The present work may provide the potential to solve the bottleneck of high efficiency DUV-LED.

Published under license by AIP Publishing. https://doi.org/10.1063/1.5081112

AlGaN-based deep ultraviolet light-emitting diodes (DUV-LEDs) have widespread application prospects in the fields of sterilization, polymer curing, biochemical detection, non-line-of-sight communication, and special lighting which have received more and more attention.[1] However, the external quantum efficiency (EQE) of AlGaN-based DUV-LEDs is still relatively low (less than 10%) that is generally attributed to the low internal quantum efficiency (IQE) and low light extraction efficiency (LEE).[2] High-quality AlN and AlGaN materials are the basis for achieving high-efficiency luminescence of DUV-LEDs. For AlGaN-based DUV-LEDs, AlN is usually used as the template layer for the epitaxial of the AlGaN layer, and so, the quality of the AlN template layer is essential for epitaxial growth of high-quality AlGaN and high-efficiency DUV-LEDs.[3,4] Currently, sapphire substrates are the primary substrate of AlGaN-based DUV-LEDs due to the lack of other suitable substrates (cheap, high quality, large size, and homogenous substrates). But the large lattice mismatch and the thermal expansion mismatch between AlN and sapphire substrates always induce high stress and high density of dislocations, thereby reducing the internal quantum efficiency and degrading the performance of LEDs.[5]

In view of the above, many techniques have been proposed and great progress has been made in the growth of AlN templates, such as epitaxial lateral overgrowth (ELO) technology on patterned sapphire substrates (PSSs) and patterned AlN/sapphire templates including micron-sized and nano-sized

patterns. These methods demonstrate the great potential of high-quality AlN growth and have also attracted great attention.[2,6–8] Furthermore, the application of patterned substrates can not only enhance the IQE by reducing the threading dislocation density but also effectively improve the LEE of DUV-LEDs.[9–13] However, epitaxial growth of AlN on PSS is difficult. Due to the high surface adhesion coefficient, the Al atoms have a low atomic surface mobility. Besides, the bond energy of AlN is high (2.88 eV), and thus, AlN tends to have a three-dimensional island growth mode.[14] Consequently, the growth of AlN requires a much higher coalescence thickness (over $3\,\mu m$) on nano-patterned sapphire substrates (NPSSs) than on flat sapphire substrates, which means long growth time and high cost.[6]

Recently, graphene (Gr) has been proposed as a buffer layer for the growth of group-III nitrides on heteroepitaxy substrates.[15] The hexagonal arrangement of sp^2 hybridized carbon atoms of Gr is similar to the (0001) c-plane of wurtzite. Besides, the epitaxial process of group-III nitrides on Gr is not heteroepitaxy but quasi-van der Waals epitaxy (QvdWE), which has been proposed to reduce the mismatch effect.[16,17] Kim et al. have reported the direct QvdWE of high quality GaN films with low defectivity and surface roughness on epitaxial Gr.[16] Chen et al. used Gr films as buffer layers for the QvdWE of high-quality AlN and GaN films and realized the fabrication of high-performance blue LEDs.[5] However, since the surface of Gr is chemically inert, the nucleation of the group-III nitride is suppressed and the growth of high-quality nitride is limited,[15] leading to many problems for the epitaxy of the group-III nitride on Gr. Moreover, AlN epitaxy on Gr and the growth and fabrication of DUV-LEDs with the Gr interlayer are still rarely reported.

In this work, we realize a Gr-assisted rapid QvdWE of high-quality AlN thin films on NPSS. The effects of Gr on reducing the surface migration barrier and promoting the lateral migration of metal aluminum adatoms are confirmed by first-principles calculations. The AlN thin films can completely coalesce and cover the Gr/NPSS at a thickness of less than $1\,\mu m$. High-resolution X-ray diffraction (HRXRD) and Raman spectra reveal the reduced dislocation density and released biaxial stress in the AlN epilayer, respectively. The Gr/NPSS-based AlGaN DUV-LED also shows stronger electroluminescence (EL) at a peak wavelength of 280 nm under a current of 40 mA compared to that without the Gr interlayer. The Gr buffer layer provides ideas and directions for the efficient and low-cost growth of group-III nitrides and DUV-LEDs on NPSS.

The NPSS prepared by the nano-imprint lithography technique illustrates the nano-concave cone patterns as shown in Fig. 1(a) and the inset.[18] The depth, the period of pattern, and the width of the unetched regions are 400 nm, $1\,\mu m$, and 300 nm, respectively. The Gr layers are directly grown on 2-in. NPSS by catalyst-free-atmospheric-pressure chemical vapor deposition (APCVD) at 1050 °C for 3 h, under a gas mixture of 500 sccm Ar, 300 sccm H_2, and 30 sccm CH_4, to avoid complex and technically demanding transfer processes, as shown in Fig. 1(b).[5] Before the epitaxial growth of AlN, nitrogen reactive ion etching (RIE) plasma treatment with a capacitively coupled radio frequency is applied to introduce defects into the Gr film for enhancing its chemical reactivity since the epitaxial growth of AlN on the
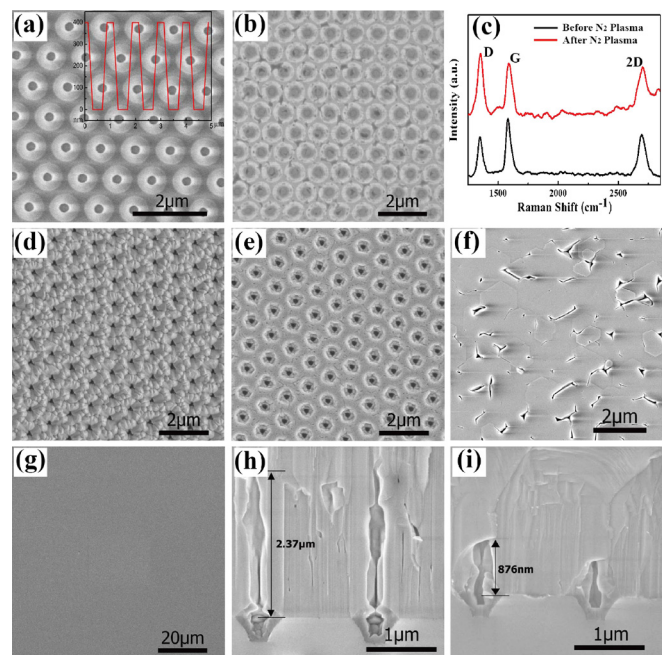

FIG. 1. (a) SEM image of the bare NPSS. The inset in (a) shows the line profile of the patterns of NPSS by AFM. (b) SEM image of the as-grown Gr films on NPSS. (c) Raman spectra of the graphene film before N_2 plasma treatment (black) and after N_2 plasma treatment (red). (d) and (f) show the SEM images of the initial 10 min and 2 h growth of AlN films on NPSS without the Gr interlayer. (e) and (g) show the SEM images of the initial 10 min and 2 h growth AlN films on NPSS with the Gr interlayer. (h) and (i) show the cross-sectional SEM images of AlN films on NPSS without and with the Gr interlayer.

pristine Gr film is difficult.[5,19] The Gr/NPSS substrate is exposed to a N_2 flow rate of 300 sccm for 30 s plasma treatment with a power of 50 W before loading into the metal–organic chemical vapor deposition (MOCVD) chamber.[5] The Raman spectra in Fig. 1(c) show an obvious increase in the D peak of the plasma treated Gr compared to that of the pristine one. The intensity ratio of D peak to G peak (I_D/I_G) increases from 0.68 to 1.18, attributing to the increase in dangling bonds that are generated during the plasma treatment.[5]

For comparison, AlN films are simultaneously grown on NPSS with and without the Gr interlayer in a single experiment by MOCVD. To study the initial growth mode of AlN, the growth of AlN is carried out at 1200 °C for 10 min, with a gas mixture of 7000 sccm H_2, 70 sccm trimethylaluminum (TMAl), and 500 sccm NH_3. Meanwhile, we also grow AlN films for 2 h under the same conditions. The V/III ratio of both initial growth of 10 min and subsequent growth of 2 h is 270. Here, AlN is directly grown without using the low temperature buffer layer. As shown in Fig. 1(d), the formation of irregular AlN islands indicates that AlN exhibits a three-dimensional growth on bare NPSS. In contrast, AlN tends to grow in a lateral two-dimensional manner on the NPSS with Gr, rapidly coalesces, and covers the hole as shown in Fig. 1(e). After 2 h of growth, the surface of the AlN film grown directly on bare NPSS is rough and nonuniform [Fig. 1(f)], while the AlN film with the Gr interlayer becomes continuous

and flat [Fig. 1(g)]. The corresponding cross-sectional Scanning electron microscopy (SEM) images of AlN grown for 2 h are also shown in Figs. 1(h) and 1(i), respectively. We can clearly observe that with the assistance of the Gr interlayer, AlN has realized complete coalescence below a thickness of $1 \mu m$, which is less than half of the thickness (about $2.4 \mu m$) on bare NPSS.

The QvdWE growth of AlN on NPSS with the Gr interlayer is also expected to reduce the dislocation density and release the biaxial stress in the epilayer. Figures 2(a) and 2(b) show typical X-ray rocking curves (XRCs) of AlN films grown on NPSS with and without the Gr interlayer, respectively. The (0002) full width at half maximum (FWHM) of the X-ray ω-scan (rocking curve) of the AlN epilayer is significantly reduced from 455.4 to 267.2 arc sec with the assistance of Gr, and its $(10\bar{1}2)$ FWHM is also reduced from 689.2 to 503.4 arc sec. The estimated densities of screw and edge dislocations of as-grown AlN without Gr are 4.51×10^8 and $4.40 \times 10^9 \mathrm{cm}^{-2}$, respectively. In contrast, they are reduced to 1.55×10^8 and $2.60 \times 10^9 \mathrm{cm}^{-2}$ with the assistance of Gr, to meet the application requirement of DUV-LEDs.[20] However, growth optimization is still needed to further reduce the dislocation density. The Raman spectrum of the E_2 phonon mode of AlN that is sensitive to the stress is used to evaluate the biaxial stress.[21] With the Gr interlayer, the E_2 peak of AlN is located at $658.3 \mathrm{cm}^{-1}$, which is very close to the stress-free AlN $(657.4 \mathrm{cm}^{-1})$ as shown in Fig. 2(c), while AlN grown on the bare NPSS shows a higher frequency $(660.6 \mathrm{cm}^{-1})$ due to the high compressive strain.[22] Based on these measurements, we estimate that the residual stress of AlN is significantly reduced from 0.87 GPa to 0.25 GPa with the assistance of Gr.[23]

The high-resolution transmission electron microscopy (HRTEM) image of the AlN/Gr/NPSS interface shows the presence of an approximately 0.7-nm-thick Gr layer [dark area in Fig. 2(d)] that keeps its original layered structure after 1200 °C AlN growth owing to the excellent stability. The selected-area

electron diffraction (SAED) pattern of the AlN domain shows a single diffraction pattern of the (0001) c-axis-oriented wurtzite structure [Fig. 2(e)], while the SAED pattern from the interface region proves the orientation relationships of (0002) AlN// (0006) Al_2O_3 and $(0\bar{1}10)$ AlN//$(\bar{1}120)$ Al_2O_3 [Fig. 2(f)]. The bright-field cross-sectional TEM image of AlN grown on Gr/NPSS with $g = [0\bar{1}10]$ is shown in Fig. 2(g). The area enclosed by the red line is the underlying nano-pattern of the sapphire, and the air void above the nano-pattern is formed during the growth process. High threading dislocation density originating from the interface between AlN and Gr/NPSS is observed above the un-etched sapphire regions. Due to the lateral two-dimensional growth of AlN, the threading dislocation near the void bends and annihilates at the end of the void, thereby reducing the dislocation density of AlN. Correspondingly, the estimated dislocation density is reduced from about $5.5 \times 10^9 \mathrm{cm}^{-2}$ near the interface to $1.5 \times 10^9 \mathrm{cm}^{-2}$ on the surface, when assuming a sample thickness of $1.5 \mu m$, which is consistent with the estimation based on the X-ray ω scan (rocking curve). Therefore, the stress of the epitaxial layer is largely released, and the dislocation density of AlN grown on Gr is also reduced due to QvdWE growth.

The initial growth of AlN is closely related to the adsorption and diffusion of Al adatoms on the substrate. As is well known, the adatom mobility (diffusion rate) is related to the diffusion barrier by an Arrhenius-type exponential law

$$r = v \exp(-E_{\mathrm{diff}}/kT),$$

where E_{diff}, k, and T are the diffusion barrier, the Boltzmann constant, and the temperature, respectively.[24] In order to clarify the growth and migration process of AlN during the epitaxial on MOCVD, we perform first-principles calculations using the Vienna ab-initio simulation package (VASP)[25] to study the adsorption energy and diffusion barrier of Al adatoms. We adopt the projector-augmented wave potentials[26] and the generalized-gradient approximation of Perdew, Burke, and Ernzerhof for the exchange correlation functional.[27] The energy cutoff for the plane-wave expansion is set as 400 eV. Van der Waals interactions are included using the Becke88 optimization functional.[28] The diffusion barrier is calculated using the nudged elastic band method based on the transition state theory.[29,30] The Al-terminated Al_2O_3(0001) 2×2 surface is modeled by an eight-layer slab with the bottom layer passivated by pseudo-hydrogen atoms. The passivated pseudo-hydrogen atoms and the three bottom layers of Al_2O_3 are kept fixed during the relaxation. The adsorption and diffusion of Al adatoms on Gr are modeled on a 4×4 Gr supercell. The k-point meshes for the Brillouin zone sampling for the two systems are $4 \times 4 \times 1$ and $9 \times 9 \times 1$, respectively.[31] The atomic coordinates are fully relaxed until the Hellmann-Feynman forces on each atom are less than 0.02 eV/Å.

In bulk Al_2O_3, the two Al atoms are not co-planar, which are named as low-Al and high-Al atoms. According to previous studies, the most stable (0001) surface has only one low-Al atom which binds strongly to the sub-surface O atoms.[32] Two adsorption sites for Al adatoms are considered as shown in the inset of Fig. 3(a), the high-Al and vacancy sites, with adsorption energies of 2.69 and 1.67 eV, respectively. Our calculation shows that the
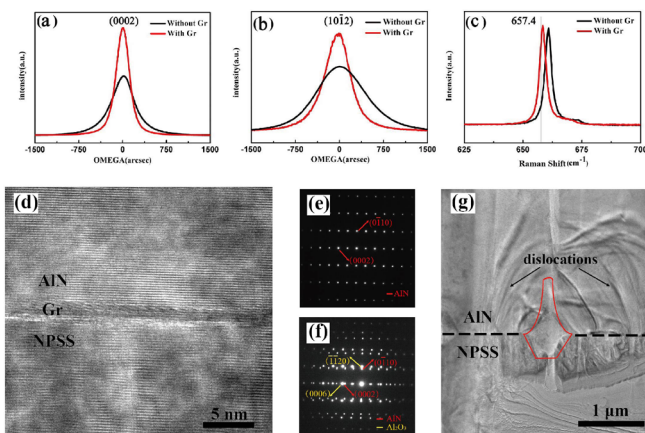

FIG. 2. XRC of (a) (0002) and (b) $(10\bar{1}2)$ for AlN films grown on NPSS with and without the Gr interlayer. (c) Raman spectra of AlN layers grown on NPSS with and without the Gr interlayer. (d) HRTEM image of the AlN/Gr/NPSS interface. (e) and (f) Show the SAED pattern taken from the AlN layer and the interface between AlN and Gr/NPSS. (g) Bright-field cross-sectional TEM images of AlN grown on Gr/ NPSS with $g = [0\bar{1}10]$.
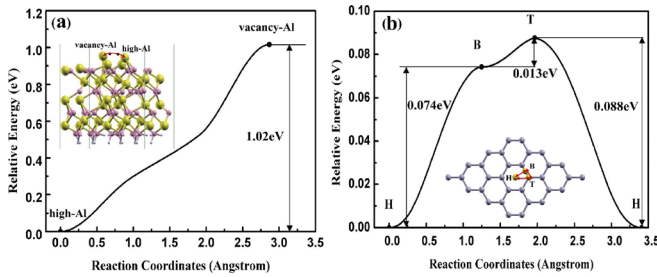
FIG. 3. (a) The diffusion barrier of the Al adatom on the Al_2O_3(0001) surface from the high-Al to vacancy sites. The inset shows the adsorption geometries of the two sites. The two small black dots indicate the intermediate sites for the Al adatom along the diffusion path. (b) The diffusion barriers of the Al adatom on the Gr surface between three adsorption sites: H site (on top of the center of a hexagonal ring), B site (on top of the center of the C–C bond), and T site (on top of a C atom). The yellow, pink, and grey balls represent the Al, O, and C atoms, respectively.

diffusion of the surface Al atom from the low-Al site to other sites is very unfavorable. Thus, the possible diffusion path of Al adatoms should be between the high-Al and the vacancy sites, with a diffusion barrier of 1.02 eV [Fig. 3(a)]. The large diffusion barrier indicates that the Al adatoms is difficult to diffuse on the Al_2O_3(0001) surface even at 1200 °C, and thus, they prefer three-dimensional longitudinal growth and form relatively discrete islands rather than large nuclei, which is consistent with our experimental observations. However, on the Gr surface, the calculated diffusion barriers between different sites (H, B, and T sites) are turned out to be less than 0.1 eV, much less than that on Al_2O_3,[33] as shown in Fig. 3(b). Such a diffusion barrier is even less than kT at the growth temperature of 1200 °C, which means that the Al adatom can diffuse almost freely on the Gr sheet. Moreover, the reactivity of Gr is greatly enhanced by introducing defects after plasma treatment, which would be beneficial for the AlN nucleation.[34] The strong binding of Al adatoms to the defect sites and the free diffusion on the non-defective regions ensure the effective nucleation and fast growth for AlN layers, as observed in our experiments.

Based on the above facts, we propose a growth model in which AlN coalesces to cover the concave pattern and grows into a thin film on Gr/NPSS and bare NPSS. Figures 4(a) and 4(b) show the schematic growth process of the AlN film on NPSS with and without the Gr interlayer, while Figs. 4(c) and 4(d)
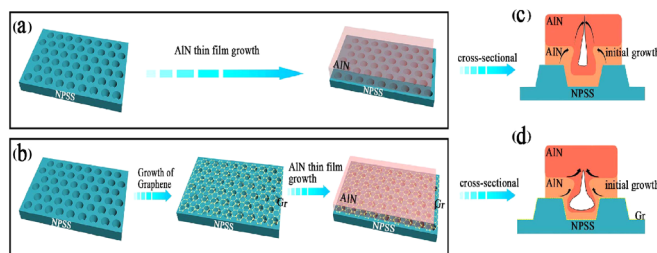
present the corresponding cross-sectional diagrams of AlN growth, respectively. As shown in Fig. 4(c), in the initial growth stage of AlN on bare NPSS, Al adatoms are difficult to diffuse rapidly because they are firmly adsorbed on the sapphire surface so that AlN presents the three-dimensional longitudinal island growth mode. Therefore, the lateral combination of the AlN nucleation islands is relatively slow and it is hard to cover the NPSS at a thin growth thickness. In contrast, on the surface of Gr/NPSS, Al adatoms have lower adsorption energy and a migration barrier,[35] which allow adatoms to diffuse easily on the substrate surface. Due to the longer diffusion length on the Gr/NPSS surface, AlN prefers the lateral two-dimensional growth mode, so that it can be rapidly and laterally coalesced, and thus, the pattern is quickly covered to form a flat AlN film during further growth, as shown in Fig. 4(d).

Finally, the AlGaN-based DUV-LEDs are grown on the AlN/Gr/NPSS and AlN/NPSS templates. The schematic structure of AlGaN DUV-LED on AlN/Gr/NPSS is shown in Fig. 5(a). A 20-period AlN (2 nm)/$Al_{0.6}Ga_{0.4}N$ (2 nm) superlattice (SL) is first deposited at 1130 °C. Then, an n-$Al_{0.55}Ga_{0.45}N$ layer with the Si concentration of 3×10^{18} cm^{-3} is deposited with the thickness of 1.8 μm. 5-period $Al_{0.4}Ga_{0.6}N$ (3 nm)/$Al_{0.5}Ga_{0.5}N$ (12 nm) multiple quantum wells (MQWs) are further grown, and the 50 nm-thick layers of the Mg-doped p-$Al_{0.65}Ga_{0.35}N$ electron blocking layer (EBL), the p-$Al_{0.5}Ga_{0.5}N$ (30 nm) cladding layer, and the 150 nm-thick p-GaN contact layer are subsequently extended with the Mg concentration of 1×10^{18} cm^{-3}. After the growth, the p-type layers are annealed at 800 °C with N_2 flow for 20 min to activate the Mg acceptors. The EL characteristics of the DUV-LEDs are evaluated as shown in Fig. 5(b). The typical EL spectrum from a DUV-LED structure with a Gr interlayer shows 2.6 times stronger luminescence at a peak wavelength of 280 nm at a current of 40 mA compared to that without the Gr interlayer, which originates from the reduced defect density. Further device results will be discussed in another paper.

In summary, we have achieved the rapid QvdWE of high quality AlN films on NPSS by using the Gr interlayer, which may bring several disruptive technologies to the traditional craft. First-principles calculations show that the introduction of the Gr interlayer significantly reduces the migration barrier of Al atoms on the surface to only 0.074 eV which is an order of magnitude lower than the migration barrier on the bare NPSS. Enhancing the lateral migration of the adatoms results in a significant reduction in the coalescence thickness of the AlN film grown on the Gr/NPSS, and such a growth process can greatly
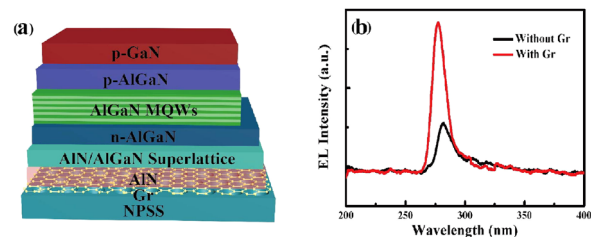

FIG. 4. Schematic diagrams of AlN growth (a) on bare NPSS and (b) on Gr/NPSS. (c) and (d) Cross-sectional schematic diagrams of AlN films grown on bare NPSS and Gr/NPSS.

FIG. 5. (a) Schematic diagram of the AlGaN-based DUV-LED structure. (b) EL spectra of the DUV-LEDs with and without the Gr interlayer.

shorten the MOCVD growth time and reduce the cost. The DUV-LED grown on Gr/NPSS also demonstrates obviously enhanced luminescence performance.

REFERENCES

[1]A. Khan, K. Balakrishnan, and T. Katona, Nat. Photonics **2**, 77 (2008).

[2]D. Lee, J. W. Lee, J. Jang, I.-S. Shin, L. Jin, J. H. Park, J. Kim, J. Lee, H.-S. Noh, Y.-I. Kim, Y. Park, G.-D. Lee, Y. Park, J. K. Kim, and E. Yoon, Appl. Phys. Lett. **110**, 191103 (2017).

[3]J. Yun and H. Hirayama, J. Appl. Phys. **121**, 013105 (2017).

[4]Y. Sakai, Y. Zhu, S. Sumiya, M. Miyoshi, M. Tanaka, and T. Egawa, Jpn. J. Appl. Phys., Part 1 **49**, 022102 (2014).

[5]Z. Chen, X. Zhang, Z. Dou, T. Wei, Z. Liu, Y. Qi, H. Ci, Y. Wang, Y. Li, H. Chang, J. Yan, S. Yang, Y. Zhang, J. Wang, P. Gao, J. Li, and Z. Liu, Adv. Mater. **30**, 1801608 (2018).

[6]P. Dong, J. Yan, J. Wang, Y. Zhang, C. Geng, T. Wei, P. Cong, Y. Zhang, J. Zeng, Y. Tian, L. Sun, Q. Yan, J. Li, S. Fan, and Z. Qin, Appl. Phys. Lett. **102**, 241113 (2013).

[7]M. Imura, K. Nakano, G. Narita, N. Fujimoto, N. Okada, K. Balakrishnan, M. Iwaya, S. Kamiyama, H. Amano, I. Akasaki, T. Noro, T. Takagi, and A. Bandoh, J. Cryst. Growth **298**, 257 (2007).

[8]V. Kueller, A. Knauer, F. Brunner, U. Zeimer, H. Rodriguez, M. Kneissl, and M. Weyers, J. Cryst. Growth **315**(1), 200 (2011).

[9]U. Zeimer, V. Kueller, A. Knauer, A. Mogilatenko, M. Weyers, and M. Kneissl, J. Cryst. Growth **377**, 32 (2013).

[10]M. Kim, T. Fujita, S. Fukahori, T. Inazu, C. Pernot, Y. Nagasawa, A. Hirano, M. Ippommatsu, M. Iwaya, T. Takeuchi, S. Kamiyama, M. Yamaguchi, Y. Honda, H. Amano, and I. Akasaki, Appl. Phys. Express **4**, 092102 (2011).

[11]C.-Y. Chang, S.-J. Chang, S. Member, C. H. Liu, S. Li, and E. Chen, IEEE Photonic Technol. Lett. **25**, 88 (2013).

[12]H. Gao, F. Yan, Y. Zhang, J. Li, Y. Zeng, and G. Wang, J. Appl. Phys. **103**, 014314 (2008).

[13]J.-K. Huang, D.-W. Lin, M.-H. Shih, K.-Y. Lee, J.-R. Chen, H.-W. Huang, S.-Y. Kuo, C.-H. Lin, P.-T. Lee, G.-C. Chi, and H.-C. Kuo, J. Disp. Technol. **9**, 947 (2013).

[14]M. Kneissl, T. Kolbe, C. Chua, V. Kueller, N. Lobo, J. Stellmach, A. Knauer, H. Rodriguez, S. Einfeldt, Z. Yang, N. M. Johnson, and M. Weyers, Semicond. Sci. Technol. **26**, 014036 (2011).

[15]K. Chung, C.-H. Lee, and G.-C. Yi, Science **330**, 655 (2010).

[16]J. Kim, C. Bayram, H. Park, C.-W. Cheng, C. Dimitrakopoulos, J. A. Ott, K. B. Reuter, S. W. Bedell, and D. K. Sadana, Nat. Commun. **5**, 4836 (2014).

[17]N. Han, T. V. Cuong, M. Han, B. D. Ryu, S. Chandramohan, J. B. Park, J. H. Kang, Y.-J. Park, K. B. Ko, H. Y. Kim, H. K. Kim, J. H. Ryu, Y. S. Katharria, C.-J. Choi, and C.-H. Hong, Nat. Commun. **4**, 1452 (2013).

[18]H.-W. Huang, J.-K. Huang, S.-Y. Kuo, K.-Y. Lee, and H.-C. Kuo, Appl. Phys. Lett. **96**, 263115 (2010).

[19]P. Gupta, A. A. Rahman, N. Hatui, M. R. Gokhale, M. M. Deshmukh, and A. Bhattacharya, J. Cryst. Growth **372**, 105 (2013).

[20]H. Heinke, V. Kirchner, S. Einfeldt, and D. Hommel, Appl. Phys. Lett. **77**, 2145 (2000).

[21]V. Lughi and D. R. Clarke, Appl. Phys. Lett. **89**, 241911 (2006).

[22]T. Prokofyeva, M. Seon, J. Vanbuskirk, M. Holtz, S. A. Nikishin, N. N. Faleev, H. Temkin, and S. Zollner, Phys. Rev. B **63**, 125313 (2001).

[23]Y. Li, Y. Zhao, T. Wei, Z. Liu, R. Duan, Y. Wang, X. Zhang, Q. Wu, J. Yan, X. Yi, G. Yuan, J. Wang, and J. Li, Jpn. J. Appl. Phys., Part 1 **56**, 085506 (2017).

[24]W. Zhu, F. Buatier de Mongeot, U. Valbusa, E. G. Wang, and Z. Zhang, Phys. Rev. Lett. **92**, 106102 (2004).

[25]G. Kresse and J. Hafner, Phys. Rev. B **47**, 558(R) (1993).

[26]P. E. Blöchl, Phys. Rev. B **50**, 17953 (1994).

[27]J. P. Perdew, K. Burke, and M. Ernzerhof, Phys. Rev. Lett. **77**, 3865 (1996).

[28]J. Klimeš, D. R. Bowler, and A. Michaelides, Phys. Rev. B **83**, 195131 (2011).

[29]G. Mills, H. Jónsson, and G. K. Schenter, Surf. Sci. **324**, 305 (1995).

[30]G. Henkelman, B. P. Uberuaga, and H. Jónsson, J. Chem. Phys. **113**, 9901 (2000).

[31]H. J. Monkhorst and J. D. Pack, Phys. Rev. B **13**, 5188 (1976).

[32]X. G. Wang, A. Chaka, and M. Scheffler, Phys. Rev. Lett. **84**, 3650 (2000).

[33]Y. Alaskar, S. Arafin, D. Wickramaratne, M. A. Zurbuchen, L. He, J. McKay, Q. Lin, M. S. Goorsky, R. K. Lake, and K. L. Wang, Adv. Funct. Mater. **24**, 6629 (2014).

[34]Z. Y. A. Balushi, T. Miyagi, Y.-C. Lin, K. Wang, L. Calderin, G. Bhimanapati, J. M. Redwing, and J. A. Robinson, Surf. Sci. **634**, 81 (2015).

[35]K. T. Chan, J. B. Neaton, and M. L. Cohen, Phys. Rev. B **77**, 235430 (2008).